Chapter-2

Localized Surface Plasmon Resonance based Sensing and Biosensing Investigation

Sibasish Dutta

Department of Physics,Tezpur University, 784028 Assam India
E-mail: dutta.sibasish94@gmail.com

The present chapter provides an overview of Localized Surface Plasmon Resonance (LSPR) phenomena associated with noble metal nanoparticles. The physics and analytical theory describing the LSPR phenomena have been discussed in detail. Further, the variation of peak resonance wavelength and its dependency on different parameters of the nanoparticles have been presented. Finally, different types of LSPR configurations along with LSPR based multiplexing for various sensing and biosensing investigations have been briefly discussed.

1. INTRODUCTION

Colloidal nanoparticles and related chemistry have undergone significant growth over a period of three decades [1]. Noble metal nanoparticles of

gold, copper, silver and aluminium were used whose records can be traced back to 4th century A.D. The utilization of colloidal gold nanoparticles (AuNPs) can be dated back to medieval period when they were used as colouring pigment. In the early twentieth century, many scientists have contributed towards synthesis mechanisms of variety of AuNPs [2]. One of the most famous utilization of noble metal nanoparticles can be seen in Lycurgus cup, which exhibits vibrant colors due to composition of gold and silver nanoparticles in it. At nanoscale, a vast change in the optical properties occurs for metals that become more pronounced when the size of the nanoparticles becomes comparable to the wavelength of the incident light. A specific type of metal nanoparticles can display different colors just by changing its size. The strong colours of noble metal nanoparticles are attributed to their intense absorption and scattering properties when light is incident on them and the related phenomena is termed as localized surface plasmon resonance (LSPR). In the present chapter, a comprehensive review of localized surface plasmon resonance has been presented. The chapter covers an analytical review of LSPR theory, LSPR based sensing, sensitivity of LSPR sensors and dependence of its selectivity on various factors. Finally, an extensive review of LSPR based biological sensing applications have been discussed.

2. THE PHYSICS OF LOCALIZED SURFACE PLASMON RESONANCE: BULK, SURFACE AND LOCALIZED SURFACE PLASMONS

A plasmon is a quantum of plasma oscillation when collective oscillation of free electrons of noble metals occurs. One can visualize the oscillation of

plasmons in terms of oscillations of electron gas relative to fixed ionic cores due to the presence of external electric field. The oscillation of electron gas for bulk plasmons occur at plasma frequency having energy given as:

$$E_p = \frac{h}{2\pi}\sqrt{\frac{ne^2}{m\epsilon_0}} \quad (1)$$

where ε_0 is the permittivity of free space, n is the electron density, e is the charge of electron and m is its mass.

On the surface of metal, when oscillation of electron density occurs due to incident transverse magnetic or p-polarized light, then excitation of plasmons takes place which is termed as surface plasmons or surface plasmon polaritons (SPP). SPPs are propagating surface electromagnetic wave when the incident light undergoes resonance with respect to the conduction electrons of the metal. The resonance is achieved when both the momentum and energy of the incident light matches to that of the plasmons. At this point, a strong absorption of incident radiation occurs which falls in visible or NIR region of the electromagnetic spectrum for most of the noble metals.

When the plasmon oscillation is confined within the dimension of metal nanoparticles, then it is termed as localized surface plasmon. When electromagnetic radiation is incident on the nanostructures, and then it can induce collective oscillation of conduction electrons provided, the wavelength of the incident light is comparable to that of the nanostructures. The resonance condition is achieved when the frequency of the incident radiation matches with that of the frequency of the oscillating electrons. At resonance, the incident radiation undergoes resonance coupling with the

nanoparticles as a result of which the electromagnetic field at the vicinity of the nanoparticles gets enhanced. Unlike surface plasmons, localized surface plasmons are non-propagating in nature and mainly confined within the vicinity of the nanoparticle. The complete theory of localized surface plasmons can be understood in terms of Mie theory, which has been discussed in the next section.

2.1 Mie theory of scattering

The simplest example of Mie theory [3] can be understood using a spherical metallic nanoparticle of radius r, embedded in a medium of real refractive index ε_m. Solving the Maxwell's equation for scattering and absorption of light by small particles, one can obtain the analytical solutions. When a plane incident wave is scattered by a homogenous conducting sphere, the scattering, absorption and extinction cross-sections [4] are given by:

$$\sigma_{sca} = \frac{\lambda^2}{2\pi} \sum_{n=1}^{\infty}(2n+1)\{|a_n|^2 + |b_n|^2\} \quad (2)$$

$$\sigma_{ext} = \frac{\lambda^2}{2\pi} \sum_{n=1}^{\infty}(2n+1)Real\{a_n + b_n\} \quad (3)$$

Here k represents wave vector of the incident wave, L represents integers for diople, quadrupole and higher multipoles for scattering. While a_n and b_n represents the expansion coefficients for the scattered wave.

For small particle approximation (i.e. particle diameter < 10 nm),

$$\sigma_{sca} = \frac{32\pi^4\epsilon_m^2}{\lambda^4} V^2 \frac{(\epsilon_1-\epsilon_m)^2+(\epsilon_2)^2}{(\epsilon_1+2\epsilon_m)^2+(\epsilon_2)^2} \quad (4)$$

$$\sigma_{ext} = \frac{18\pi\epsilon_m^{3/2}}{\lambda} V \frac{\epsilon_2(\lambda)}{[\epsilon_1(\lambda)+2\epsilon_m]^2+[\epsilon_2(\lambda)]^2} \quad (5)$$

ISBN: 978-93-85822-38-4

In order to have the maximum extinction cross-section, the denominator of equation (5) should be minimum and it can happen when $\epsilon_1 = -2\epsilon_m$. Hence it can be said that peak extinction coefficient for LSPR depends on the dielectric medium of the surrounding.

3. DEPENDENCE OF LSPR ON REFRACTIVE INDEX

From the complex metal dielectric function, $\tilde{\epsilon} = \epsilon_{1 + i}\epsilon_{2,}$ where ϵ_1 represents the real part and $\epsilon_{2,}$ represents the imaginary part of the dielectric function.

From the Drude model [5],

$$\epsilon_1 = 1 - \frac{\omega_p^2}{(\omega^2 + \ ^2)} \tag{6}$$

where ω_p represents the plasma frequency and Υ, the damping parameter of the metal in bulk form.

When $\Upsilon << \omega_p$ (for visible and NIR frequencies), equation (6) reduces to

$$\epsilon_1 = 1 - \frac{\omega_p^2}{\omega^2} \tag{7}$$

Now putting the resonance condition ($\epsilon_1 = -2\epsilon_m$), the expression for ω ($=\omega_{max}$) becomes

$$\omega_{max} = \frac{\omega_p}{\sqrt{2\epsilon_m + 1}} \tag{8}$$

here ω_{max} is the resonance frequency.

Substituting the value of $\epsilon_m = n^2$ in equation no. (8) the above equation can be expressed in terms of wavelength as

$$\lambda_{max} = \lambda_p\sqrt{2n_m^2 + 1} \tag{9}$$

Here λ_{max} is the LSPR peak wavelength value and λ_p represents the wavelength corresponding to the plasma frequency of bulk metal.

ISBN: 978-93-85822-38-4

From the relation (9) It is clear that LSPR peak wavelength value varies almost proportional to that of refractive index of the surrounding dielectric medium. Hence, it forms the basic mechanism of LSPR based sensing scheme where, a change in surrounding refractive index of the medium corresponds to a change in resonance wavelength value for the nanoparticles.

With change in refractive index of the surrounding medium, the corresponding spectral shift of LSPR resonance wavelength can be explained by the following expression [6]:

$$\Delta\lambda \approx m(n_{adsorbate} - n_{medium})\,(1-e^{-2d/l_d}) \qquad (10)$$

where, m denotes the sensitivity factor, in terms of nm per refractive index unit. $n_{\text{adsorbate}}$ and n_{medium} represents the refractive index of the analyte and refractive index of the surrounding medium respectively.

4. COMPARISON OF SURFACE PLASMON RESONANCE (SPR) AND LOCALIZED SURFACE PLASMON RESONANCE (LSPR) SENSING

SPR and LSPR sensing techniques are similar in the sense that in both the techniques, the plasmons interact with the external dielectric medium, corresponding to which a shift in peak resonance wavelength is observed. However, in case of LSPR, the marginal bulk effect is smaller than that of SPR. Also, the spatial resolution for LSPR is greater than that of SPR along both normal and lateral direction. Most importantly, SPR instrumentation requires precise optical alignment and hence makes the instrumentation complex to design but the same does not holds good for LSPR instrumentation. In addition, SPR sensing is affected by temperature

variation and requires precise temperature monitoring. On the other hand, the peak resonance wavelength for nanoparticles can be easily detected using a spectrophotometer and does not require precise temperature control. Due to such complexity in optical instrumentation, the price of the commercially available SPR instruments is too large. Hence, LSPR sensing instrumentation not only retains the virtue but also reduces the instrumental complexity as well as price to a considerable extent. In addition to that, the marginal bulk effect of LSPR sensing scheme allows specific detection of analytes and reduces the chances of false signal detection of undesired analytes.

5. REFRACTIVE INDEX SENSITIVITY DEPENDENCE ON SHAPE, SIZE AND MATERIAL OF NANOPARTICLES

5.1 Nanoparticle size

Mie theory of scattering explains the relation between the particle size with scattering and absorption cross-sections. When the size of the particle (of radius R) is much smaller than the wavelength of the incident light than absorption dominates over scattering. Nanoparticles whose size is less than 40 nm, the absorption cross-section for them is greater than scattering cross-section. In between 40 nm to 80 nm, the magnitude of absorption cross-section decreases and scattering cross-section increases. At about 80 nm, the magnitude of scattering cross-section becomes greater than that of absorption cross-section [7,8]. Aspect ratio is another important factor that governs the spectral shift in peak resonance wavelength. It is defined as the ratio between the length to the width of the nanoparticle. For a perfect spherical nanoparticle, aspect ratio is 1. The extinction spectrum of non-

spherical gold nanoparticles consists of both transverse as well as longitudinal plasmon mode. For Au nanorods, the transverse plasmon mode appears across the visible region and the longitudinal plasmon mode across the NIR of the electromagnetic spectrum. The transverse plasmon band is not affected by the size of the nanoparticle while the longitudinal plasmon band shows a spectral red-shift with increase in aspect ratio of the nanorod. With increase in aspect ratio of the particle, the longitudinal plasmon mode shows a linear increase in its peak LSPR wavelength. Therefore, the refractive index sensitivity is a function of aspect ratio of the nanoparticles and hence, higher aspect ratio favors greater spectral shift due to change in refractive index of the surrounding.

5.2 Nanoparticle shape

The shape of the nanoparticles also plays an important role in determining sensitivity. It has been observed that nanoparticles having sharp tips cause higher refractive index sensitivities. It is so because sharp tips indicate greater aspect ratio for the nanoparticles. Mock et al. reported the change in LSPR properties of silver nanoparticles with change in their shapes in the form of spheres, triangles and cubes. From the study, it has been estimated that silver nanotriangles possessed the highest sensitivity of 350 nm/RIU than nanospheres (160 nm/RIU) [9]. Since nanotriangles and nanobipyramids have sharp tips, they possess higher refractive index sensitivity [10,11]. Table 1 summarizes the refractive index sensitivities in terms of spectral shifts of different shaped gold and silver nanoparticles.

Table 1: Spectral-shift of different nanostructures

Groups	Nanoparticles	LSPR wavelength (nm)	Spectral shift (nm)
Sherry et al. [12]	Silver cube-sub	430	118
Sherry et al.[12]	Silver nanocube	510	146
Mock et al. [9]	Silver nanosphere	520	160
Underwood et al.[13]	Gold nanosphere	530	90
Malinsky et al.[14]	Silver NSL	564	191
Khalavka et al. [15]	Gold nanorattle	570	199
Raschke et al. [16]	Gold/Gold shulphide nanoshell	660	117
Nehl et al.[17]	Gold nanostar	675	238
Lee et al. [18]	Gold nanopyramid	680	221
Burgin et al.[10]	Gold bipyramid	681	352
Mayer et al. [1]	Gold nanorod	720	170
Mock et al.9	Silver nanotriangle	760	350
Nehl et al. 17	Gold nanostar	770	665

From the table it is clear that Au nanostars structures produce the highest refractive index sensitivities.

5.3 Nanoparticle material composition

Gold nanoparticles are chemically more stable and offer better size controlled synthesis than silver nanoparticles. However, the refractive index sensitivity for silver nanoparticles is larger than gold nanoparticles. Figure 1 shows the graph demonstrating the spectral shift in peak resonance wavelength of gold and silver nanoparticles towards similar change in

refractive index of the surrounding. From the previous section it can be observed that higher the plasmon resonance wavelength of the nanostructure, greater the refractive index sensitivity. However, the same does not hold good for certain cases. For example, the refractive index sensitivity of Au nanospheres of size 50-60 nm is 60 nm/RIU with plasmon resonance wavelength at ~ 530 nm [19]. For the same sized Ag nanospheres, the refractive index sensitivity is 160 nm/RIU with plasmon resonance wavelength at ~ 435 nm [9]. Similarly, for Au nanocubes, the refractive index sensitivity is 83 nm/RIU with plasmon resonance wavelength at 538 nm [15] while for the same sized Ag nanocubes; the refractive index sensitivity is 146 nm/RIU [12]. Hence, it is clear that the refractive index sensitivity is a function of the nanoparticle material.

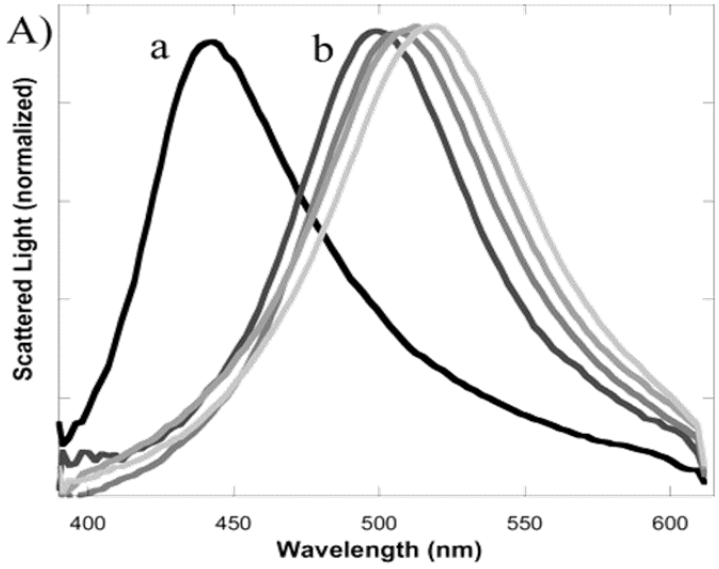

ISBN: 978-93-85822-38-4

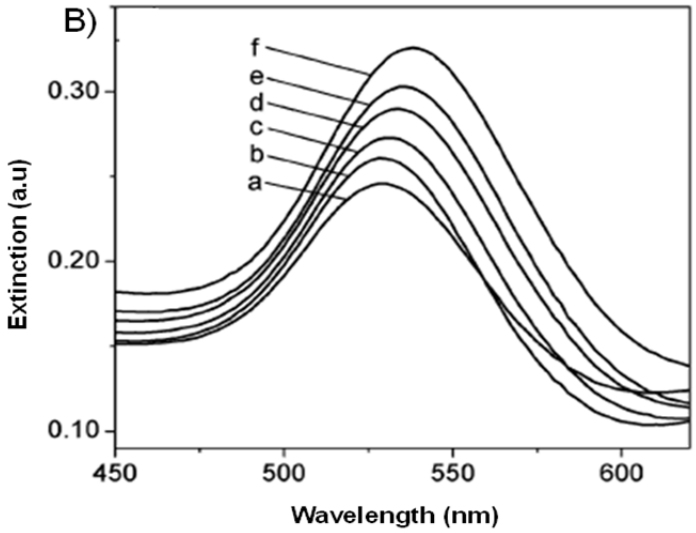

Fig. 1: Refractive index sensitivity of (A) Ag nanospheres with change in refractive index from 1.00 to 1.56 [9] and (B) Au nanospheres from 1.33 to 1.50 [19].

6. DIFFERENT TYPES OF LSPR CONFIGURATIONS

LSPR sensing technology is new as compared to SPR. LSPR sensing scheme not only preserved the virtue of SPR but also extended its scope through Surface Enhanced Raman Spectroscopy (SERS). The ease in realizing LSPR based sensors can be understood from the fact that noble metal nanoparticles (AuNPs, AgNPs etc.) can be excited directly with light that offers more flexibility in designing LSPR sensors than SPR sensors. Different types of LSPR sensors reported so far, can be broadly classified into three types:

6.1 Solution phase based LSPR

In solution phase based LSPR sensors, molecules are attached or binded to the nanoparticles directly or using specific linkers [20, 21]. Analyte

detection is done by directly putting the sample (functionalized nanoparticles) into a cuvette and capturing the transmission spectrum of the same using a standard UV-VIS spectrophotometer. The sensing is done based on the change in local refractive index of the surrounding medium of the nanoparticles as well as based on aggregation of nanoparticles. Depending on the number of binding sites of the target molecule, AuNPs get attached to them. If the target molecule has only one binding site, then, only one AuNP will be attached to it. When there are more than one binding site on the target molecule, then, there can be multiple attachment of AuNPs with the target molecule. As a result, it leads to the aggregation of the nanoparticles resulting into a change in color that can be identified through naked eye qualitatively or using a spectrophotometer quantitatively.

6.2 Substrate based LSPR

In substrate based LSPR sensors [22, 23], AuNPs are immobilized on the surface of the silica substrate which may be a glass slide or cover slip. Sometimes using electron beam lithographic technique (EBL), the nanoparticles are grown on the subtrate's surface directly. AuNP (colloidal) layer can be deposited on the surface of the substrate by various methods as follows:

(i) ***Electrostatic method***: In this method, the substrate is dipped into a polyelectrolyte solution so that the surface of the substrate attains a charge opposite to that of the AuNPs. Thereafter to deposition of AuNPs can be done by simply immersing the substrate into the AuNPs colloidal solution. Due to electrostatic force of attraction, the AuNPs get attached to the

substrate and we can get an LSPR substrate. The demerits of this technique are poor stability and uniformity.

(ii) ***Self assembled monolayer (SAM)***: SAM can also be employed for deposition of AuNPs on the substrate. Here, the surface is at first soaked in 3-aminopropyltriethoxysilane (APTES) solution in order to form thiol-terminated or amine-terminated saline SAM on the surface of the substrate. Thereafter, the APTES substrates are dipped in AuNP colloidal solution for ~ 2 hours to produce the first layer of the nanoparticles via covalent bond or electrostatic bond. The LSPR absorbance spectrum of AuNP coated substrate can be studied in transmission mode using a standard UV-VIS spectrophotometer.

6.3 Fiber optics based LSPR sensor

Fiber optics based LSPR sensors have been reported for the past 13 years to demonstrate myriad of applications for various sensing research [23, 24]. In general, the optical fiber based LSPR sensors are designed by decladding a certain portion of the core of the fiber and immobilizing AuNPs on it. The immobilization method for AuNP deposition on the surface of the fiber is similar as explained in the previous section 6.2. The AuNP coated region of the fiber constitutes the probe region or sensing head of the sensor. The probe region of the fiber may be straight, U-bend, tapered tip, and biconical tapers [25]. Light from a polychromatic source is allowed to pass through the fiber so that the evanescent field of the light can excite the localized surface plasmons (LSP) of the nanoparticles at the core-metal layer interface. This evanescent field coupling with the LSPs depends on different

parameters such as fiber geometry, incident light and metal-dielectric properties.

7. MECHANISM OF LSPR-BASED SENSING

Sensing and biosensing using LSPR can be realized in two types of sensing scheme namely, refractive index change and nanoparticle aggregation. The resonance wavelength of metal nanoparticles are sensitive to change in refractive index of the surrounding medium based on which different types of LSPR biosensors have been proposed.

7.1 Sensing based on change in refractive index

Nath et al. reported the first ever substrate based LSPR biosensor for detection of streptavidin based on biotin-streptavidin interaction. The sensing chip was prepared by depositing AuNPs on the surface of the coverslip, treated with APTES solution and after which the AuNPs were functionalized using biotin. Biotin has strong affinity for streptavidin that forms a strong and specific binding between biotin and streptavidin. Biotin is a small organic molecule that can bind itself to the surface of the nanoparticle. On the other hand, streptavidin is a larger molecule which can be easily conjugated to the biotin molecules. Since the refractive index of streptavidin is higher, so its conjugation with biotin can bring a well detectable change in resonance wavelength of the biotin conjugated AuNPs immobilized on the substrate. Several research groups have reported the interaction of biotin and streptavidin on AuNPs [markinos, hiep, harnandes]. The amount of streptavidin conjugation on biotin can be quantified by studying the shift in plasmon resonance wavelength when

streptavidin molecule binds to biotin using a standard UV-VIS spectrophotometer. Further optimization of AuNP size can significantly improve the limit of detection (LOD) of the sensing system. Chen et al. [26] reported a gold nanorod (AuNRs) based sensing strategy for studying biotin-streptavidin interaction where, AuNRs were immobilized on a glass slide that was initially treated with MPTMS. Thereafter, the substrate was modified with biotin followed by conjugation of streptavidin with the biotin molecules. An LOD of 0.42 nM is reported which is five times higher than that of Au nanospheres. The optical fiber based LSPR biosensor could detect streptavidin concentration as low as 98 pM [27]. The utility of LSPR based sensors have also been reported for antigen-antibody interaction that find numerous applications in biological immunoassay activities.

7.2 LSPR sensing based on aggregation of plasmonic nanoparticles

Noble metal nanoparticles are dispersed in a solution medium and constitute a colloidal solution which is stable. Aggregation of these nanoparticles results in a change in colour that can be observed through naked eye. This approach is very useful for visual detection of target analyte in a sample and finds a wide range of applications in the field of food, biomedical and environmental sensing research. Aptamer conjugated AuNPs of size 20 nm has been reported for colorimetric detection of cancerous cells. The target cancer cells caused change in colour from red to blue while non-cancerous cells did not produce any color change of the nanoparticle samples. Similarly, aptamer conjugated AuNPs have also been reported for colorimetric detection of thrombin [28] and quantification of mercury

concentration in water samples [29]. AuNPs have also been used for detection of DNA hybridization by functionalizing the AuNPs with thiolated non-complementary oligonucleotide. AuNPs aggregation based biological sensing has also been reported for detection of Protein kinase A (PKA), Human estrogen receptors (hERs), Lysozyme (Lysz), Trypsin (Tryp) and inhibitors [30].

Multiplxeing in LSPR based sensors

LSPR based multiplexing has been reported by Wang et al. [1] In their work, AuNRs of three different aspect ratios were functionalized with three different antibodies and then mixed together. On observing the LSPR absorption spectra, three distinguishable longitudinal plasmon bands were found. In their work, they have chosen E.Coli and Salmonella as target analytes and allowed to interact with the mixture. Owing to specific binding of these bacteria with specific antibody, two different red-shift have been observed corresponding to two different bacteria. While the third plasmonic band shows a small red-shift due to non-specific binding. Using similar strategy, Yonzon et al. [31] demonstrated a chip-based LSPR sensor by depositing silver nanotriangles of two dissimilar size with resonance wavelength at 683 nm and 725 nm. The nanotriangles were functionalized with mannose and galactose respectively and allowed to interact with Concanavalin A (ConA). Due to selective binding, only mannose coated nanotriangles (resonance wavelength at 683 nm) showed red-shift while there was no spectral shift observed for galactose coated nanotriangles

(plasmon resonance wavlength at 725 nm). Hence, LSPR multiplexing allows multiple target detection at the same time.

8. CONCLUSIONS

LSPR based sensors are emerging out as a powerful tool in different areas of sensing be it chemical or biological. In the given review work, a comprehensive study has been done on LSPR based sensing and its potential implications in developing real-time sensors. At present, localized surface plasmon based sensing can be done using spectrophotometers by capturing the modulated light passed through the nanoparticle sample solutions. The spectrophotometers can detect change in intensity of absorption as well as spectral shift of the resonance wavelength of the nanoparticles with change in concentration of the target analytes effectively. However, such techniques are restricted to laboratory settings and cannot be implemented in remote locations or outside the laboratory. In addition to that, bulky and expensive instrumentations further restrict their usage for in-field sensing applications. These issues have been addressed to a considerable extent by recent development of smartphone platform LSPR sensors as reported by different research groups [32, 33]. Here the smartphone is used as transducer that collects the modulated light signal either by using the camera or ambient light sensor of the phone. Also, the recorded signal can be processed using the existing computational platform of the smartphone and the information can be transmitted to any part of the world through the existing cellular network connectivity of the phone. Such

approaches have not only improved the portability and reduced the cost but also facilitate easy data sharing and transmissions.

The LSPR sensing technique is one of the most effective and successful label-free technique in the history of sensing technology. However, this technique itself suffers from non-specificity in target molecule detection. The reason is attributed to its sensitivity towards change in refractive index of the surrounding medium. The specificity can be achieved with specific linkers or via antigen-antibody recognition mechanisms.

REFERENCES:

[1] Mayer, K. M. & Hafner, J. H. *Chem. Rev.* **111,** 3828–3857 (2011).

[2] Amendola, V. & Meneghetti, M. *Phys. Chem. Chem. Phys.* **11,** 3805–3821 (2009).

[3] Mie, G. Beitr{ä}ge zur Optik tr{ü}ber Medien, speziell kolloidaler Metall{ö}sungen. *Ann. Phys.* **330,** 377–445 (1908).

[4] Bohren, C. F. & Huffman, D. R. John Wiley & Sons, 2008.

[5] Maier, S. A., Kik, P. G. & Atwater, H. A. *Appl. Phys. Lett.* **81,** 1714–1716 (2002).

[6] Anker, J. N. *et al. Nat. Mater.* **7,** 442–453 (2008).

[7] Jain, P. K., Lee, K. S., El-Sayed, I. H. & El-Sayed, M. A. *J. Phys. Chem. B* **110,** 7238–7248 (2006).

[8] Brown, R. G. W. *J. Mod. Opt.* **31,** 3 (1984).

[9] Mock, J. J., Smith, D. R. & Schultz, S. *Nano Lett.* **3,** 485–491 (2003).

[10] Burgin, J., Liu, M. & Guyot-Sionnest, P. *J. Phys. Chem. C* **112,** 19279–19282 (2008).

[11] Banholzer, M. J., Harris, N., Millstone, J. E., Schatz, G. C. & Mirkin, C. A. *J. Phys. Chem. C* **114,** 7521–7526 (2010).

[12] Sherry, L. J. *et al. Nano Lett.* **5,** 2034–2038 (2005).

[13] Underwood, S. & Mulvaney, P. *Langmuir* **10,** 3427–3430 (1994).

[14] Duval Malinsky, M., Kelly, K. L., Schatz, G. C. & Van Duyne, R. P. *J. Phys. Chem. B* **105,** 2343–2350 (2001).

[15] Khalavka, Y., Becker, J. & Sonnichsen, C. *J. Am. Chem. Soc.* **131,** 1871–1875 (2009).

[16] Raschke, G. *et al. Nano Lett.* **4,** 1853–1857 (2004).

[17] Nehl, C. L., Liao, H. & Hafner, J. H. *Nano Lett.* **6,** 683–688 (2006).

[18] Lee, J., Hasan, W. & Odom, T. W. *J. Phys. Chem. C* **113,** 2205–2207 (2009).

[19] Sun, Y. & Xia, Y. *Anal. Chem.* **74,** 5297–5305 (2002).

[20] Gole, A. & Murphy, C. J. *Langmuir* **21,** 10756–10762 (2005).

[21] Liao, H. & Hafner, J. H. *Chem. Mater.* **17,** 4636–4641 (2005).

[22] Huang, H. *et al. Biosens. Bioelectron.* **24,** 2255–2259 (2009).

[23] Kajikawa, K. & Mitsui, K. in *Optics East* 494–501 (2004).

[24] Mitsui, K., Handa, Y. & Kajikawa, K. *Appl. Phys. Lett.* **85,** 4231–4233 (2004).

[25] Paul, D., Dutta, S. & Biswas, R. *J. Phys. D. Appl. Phys.* **49,** 305104 (2016).

[26] Chen, C.-D., Cheng, S.-F., Chau, L.-K. & Wang, C. R. C. *Biosens. Bioelectron.* **22,** 926–932 (2007).

[27] Cheng, S.-F. & Chau, L.-K. *Anal. Chem.* **75,** 16–21 (2003).

[28] Wei, H., Li, B., Li, J., Wang, E. & Dong, S. *Chem. Commun.* 3735–3737 (2007).

[29] Li, L., Li, B., Qi, Y. & Jin, Y. *Anal. Bioanal. Chem.* **393,** 2051–2057 (2009).

[30] Vilela, D., González, M. C. & Escarpa, A. *Anal. Chim. Acta* **751,** 24–43 (2012).

[31] Yonzon, C. R. *et al. J. Am. Chem. Soc.* **126,** 12669–12676 (2004).

[32] Dutta, S., Saikia, K. & Nath, P. *RSC Adv.* **6,** 21871–21880 (2016).

[33] Fu, Q. *et al. Lab Chip* **16,** 1927–1933 (2016).